Reaction mechanism of conversion of Ɣ-valerolactone (GVL) over a Ru catalyst: a first-principles study

Reda M. Bababrik, Bin Wang*, Daniel E. Resasco
School of Chemical, Biological and Materials Engineering and Center for Interfacial Reaction Engineering (CIRE), University of Oklahoma, Norman, OK 73019
Email: wang_cbme@ou.edu

Abstract:
Conversion of biomass-derived gamma-valerolactone (GVL) to valuable chemicals has been studied extensively, and understanding the reaction mechanism is very valuable for enhancing the turnover rate and selectivity. Here, we report first-principles density functional calculations, through which we show in detail the reaction pathways of GVL conversion on a Ru(0001) surface, in good agreement with recent experimental results performed on supported Ru catalysts. We find that GVL undergoes a ring-opening reaction rather easily, and that the rate-limiting step towards the formation of 1,4-pentanediol and 2-pentanol is the hydrogenation step. The high energy barrier for this step is caused by a strong interaction between Ru and the unsaturated acyl intermediate that is formed after opening the ring. Among all the primary products, formation of the 2-butanol has the smallest activation barrier, while the slowest step is the C-C bond cleavage in the decarbonylation step. We further show that the same acyl intermediate after ring opening of GVL can also be formed by dehydrogenation of 1,4-pentanediol with a moderate activation barrier, which suggests both 2-pentanol and 2-butanol can also be produced in secondary steps.

Introduction

Renewable oxygenates derived from lignocellulosic biomass have attracted extensive attentions, because they can be converted to valuable chemicals or blended into fuels[1-7]. Among a variety of these biomass-derived oxygenates, ϒ-valerolactone (GVL) has been particularly interesting because of its excellent properties as solvent of biomass-derived streams[8,9] and the possibility of being used as a precursor for high-value chemicals[10,11]. GVL can be produced via a multi-step process in which acid catalysts convert sugars into levulinic acid, followed by noble-metal-catalyzed reduction reaction in the presence of H_2[12-14]. In addition, GVL can be converted from furfural, which is also an important platform chemical obtained from thermal treatment of biomass at moderate temperatures via dehydration of xylose[15-18]. It has been reported that conversion of furfural to GVL can be catalyzed by zeolites with Brønsted and Lewis acid sites, combined with sequential transfer-hydrogenation[19].

GVL can be converted to a variety of chemicals, such as liquid alkenes through an integrated catalytic system[10,20]. Hydrogenation of GVL over Cu-Cr oxide at 240-260 °C produces 1,4-pentanediol (1,4-PDO) and 2-methyltetrahydrofuran (2-MTHF)[21]. The former one can be potentially used as a monomer to produce biomass-derived biodegradable polymers and the latter has been identified as a fuel component[13]. The chemical conversion of GVL may involve a multi-step process including ring opening, hydrogenation and dehydration[22]. Significant efforts have been focused on the use of ruthenium catalyst, with either homogeneous molecular catalysts[22] or supported nanoparticles[23-25], with and without a solvent environment. Using a molecular Ru catalyst, by tuning the ligands and the additives in the solution, Geilen et al. have shown that the selectivity of GVL conversion can be controlled to either high-yield of 1,4-PDO or high-yield of 2-MTHF[22]. Using heterogeneous Ru/C catalysts, Al-shaal et al. have shown that, in a solvent-free environment, GVL can be converted to a mixture of 2-MTHF, 2-butanol (2-BuOH) and small amounts of 2-pentanol (2-PeOH). They proposed that the formation of 1,4-PDO is the rate-determining step in the hydrogenation of GVL[23]. Very recently, Rozenblit et al. have investigated the aqueous-phase conversion of GVL over a Ru/C catalyst, and proposed that GVL might be converted to 1,4-PDO, 2-BuoH and 2-PeOH in parallel paths derived

from the same surface acyl species produced through the ring-opening reaction[24]. In the same study, it was shown that the major product 2-BuOH results from the direct decarbonylation of the acyl species. Several elementary steps, including the ring opening and decarbonylation have been studied using DFT calculations[24]. However, a detailed reaction profile has not been investigated, and it is still not clear what are the rate-limiting steps to form the various products observed, such as 1,4-PDO, 2-BuOH and 2-PeOH.

Here we report a complete reaction profile obtained using DFT calculations, through which we show several missing links in the previously proposed reaction mechanisms of GVL ring-opening and hydrogenation reactions. We have found that hydrogenation of the unsaturated acyl species formed after the ring-opening reaction of GVL is the rate limiting step for the reaction path towards 1,4-PDO, and 2-PeOH due to the strong interaction between the Ru surface and the O and C atoms in the acyl species. By contrast, the rate-limiting step for the formation of 2-BuOH is the decarbonylation step. Formation of 2-BuOH has the lowest overall reaction barrier. In addition, we show that both 2-BuOH and 2-PeOH can be formed from the same acyl intermediate, which can also be formed through dehydrogenation of 1,4-PDO. In other words, 2-BuOH and 2-PeOH can be both primary and secondary products in the conversion of GVL over a ruthenium catalyst. Finally, we provide a discussion about how these calculations can be used to interpret relevant experimental results recently reported in the literature.

Computational Methods

DFT calculations were carried out using the VASP package[26]. The Perdew-Burke-Ernzerhof generalized gradient approximation exchange-correlation potential (PBE-GGA)[27] was used, and the electron-core interactions were treated in the projector augmented wave (PAW) method [28,29]. Structures were optimized until the atomic forces were smaller than 0.02 eV $Å^{-1}$ with a kinetic cut off energy of 400 eV. The brillioun zone was sampled using the k-point gamma for all calculations. The trend remained the same when the k-point sampling was increased to a 2*2*1. Van der Waals interactions were taken into account by incorporating the DFT-D3 semi-

empirical method[30], which significantly improves the calculation accuracy of weak adsorption systems[31]. Reaction barriers were determined with the Nudged Elastic Band method[32,33]. The Ru(0001) surface was used for the calculations due to its low surface energy[34], and was modeled with a (6×6) supercell, which contained repeated slabs with four metal layers separated by an 18 Å vacuum region. The bottom two Ru layers are fixed at their bulk positions while the top two layers are fully relaxed.

Results and Discussion:

We computed several different adsorption geometries of GVL on Ru(0001) to determine the most stable structure. It was found that GVL adsorbs on the metal surface through the carbonyl carbon, carbonyl oxygen, as well as the oxygen of the furanic ring. The carbonyl carbon binds to an hcp (hexagonal closed packed) site of the Ru(0001) surface through interaction with 3 surface ruthenium atoms with a distance of 2.19 Å. Both the carbonyl oxygen and the furanic ring oxygen bind to a surface Ru atom with distances of 2.05 Å and 2.21 Å, respectively. This adsorption configuration is in agreement with a previous calculation[24]. GVL adsorbed with this structure can undergo a ring-opening reaction with an activation barrier of 25 kJ/mol, as discussed below in Figure 1. In addition, we find an almost equally stable structure (less stable by 0.6 kJ/mol), which is shown in Figure S2, in which the carbonyl oxygen binds to a surface Ru atom with a bond length of 2.27 Å along with the methyl group pointing towards the surface. The GVL molecule adopting this configuration needs to overcome an activation barrier of 69 kJ/mol of the ring-opening reactions (Figure S3). Considering the similar adsorption energy between these two structures, we think they may reach equilibrium at the surface and the one with the lower activation barrier will dominate the surface reactions, while the second adsorption configuration may not be kinetically relevant.

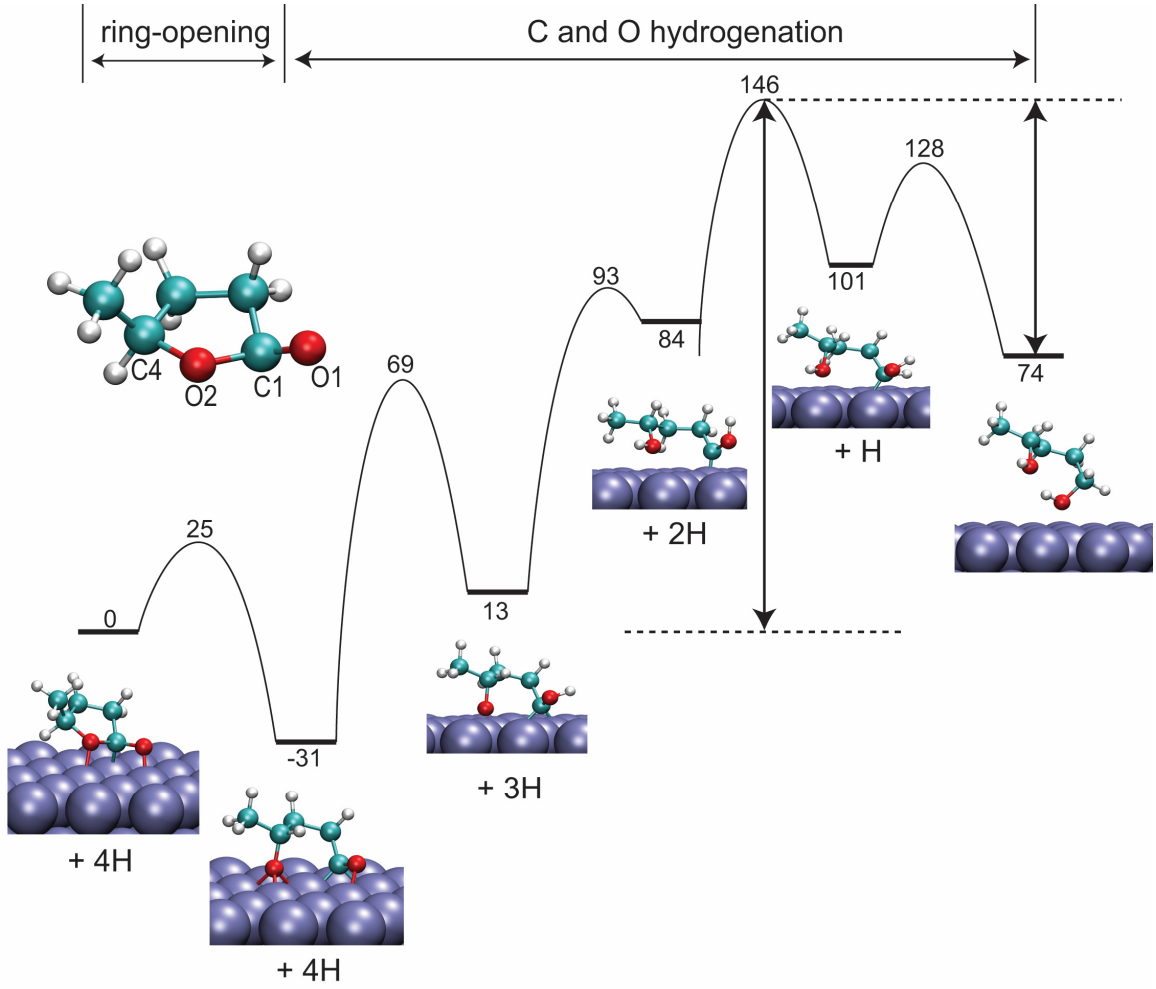

Figure 1 Energy profile calculations (kJ/mol) for the formation of 1,4-PDO from GVL. Structures of the initial, intermediate and final states are shown. The two arrows indicate the apparent barriers for the forward and backward reactions. The inset shows the gas phase GVL molecule, with the atoms labeled for discussion in the text.

In order to understand the reaction steps that GVL can undergo based on the products, detailed step-by-step reaction pathways were developed. Figure 1 shows that GVL can undergo a ring opening step, forming a surface adsorbed acyl species. This exothermic ring-opening reaction (-31 kJ/mol) is driven by the strong Ru interaction to both carbon and oxygen[35], which also drives ring-opening reactions of other heterocyclic aromatics such as furanics[36]. The combination of low energy barrier and exothermicity of this step suggest that adsorbed GVL molecules on Ru(0001) may undergo ring opening easily through the breaking of the C(1)-O(2) bond. Alternatively, the GVL ring could open at the C(4)-O(2) bond. However, Rozenblit et al. has shown that ring opening of GVL through breaking the C(4)-O(2)

bond has a much greater energy cost.[24] Moreover, the cleavage of the C(1)-O(2) bond gives a much better agreement with the product distribution found in varied experiments[23,24] than the C(4)-O(2) cleavage.

This ring-opening reaction leads to an acyl intermediate, which can go through four sequential hydrogenation steps to yield 1,4-PDO. The subsequent steps for the formation of 1,4-PDO are the hydrogenation of the two oxygen atoms followed by two hydrogenation steps of the carbonyl carbon. The first hydrogenation step occurs at the carbonyl oxygen atom - O(1) - with a true energy barrier of 100 kJ/mol. Hydrogenation of the other oxygen atom O(2) as the first step was also considered, but calculations show a higher activation barrier for this route, due to the fact that O(1) is adsorbing on a top site of the Ru surface compared to the O(2) atom, which is adsorbed on a fcc (face centered cubic) site. The reaction to form 1,4-PDO from GVL is endothermic with reaction energy of 74 kJ/mol and an apparent barrier of 146 kJ/mol. The rate limiting step is the hydrogenation step due to the strong interaction between Ru and the unsaturated carbon and oxygen atoms in the GVL ring-opening product[35], which suggests that the formation of 1,4-PDO is very sensitive to the hydrogen coverage. The energy barriers reported in figure 1 correspond to calculations done in vacuum, experimental results we carried in the presence of solvent water. As studied by Iglesia and coworkers *(Mechanistic role of water on the rate and selectivity of Fischer-Tropsch synthesis on ruthenium catalysts)*, water solvent can help stabilize intermediates through hydrogen bonding and lower the barrier for the hydrogenation steps involving the formation of O-H. However, we believe the trend and the rate determining step should hold correct. Coverage affect has been studied by Vlachos and coworkers *(Coverage-induced conformational effects on activity and selectivity: Hydrogenation and decarbonylation of furfural on Pd(111))*, where they showed that hydrogen coverage affects both the intermediates and transition states energies as well as the activation energy for hydrogenation of furfural on Pd (111) surface. This result is supported by the enhanced yield measured experimentally when increasing H_2 pressure[24]. The energy profile in Figure 1 also shows a moderate activation barrier for the reverse reaction, that is, dehydrogenation of the 1,4-PDO to form the ring-opening acyl intermediate. As discussed later in the

text, this ring-opened GVL can lead to formation of 2-BuOH and 2-PeOH. In other words, 2-BuOH and 2-PeOH may be formed either as a primary product from GVL or a secondary product via 1,4-PDO.

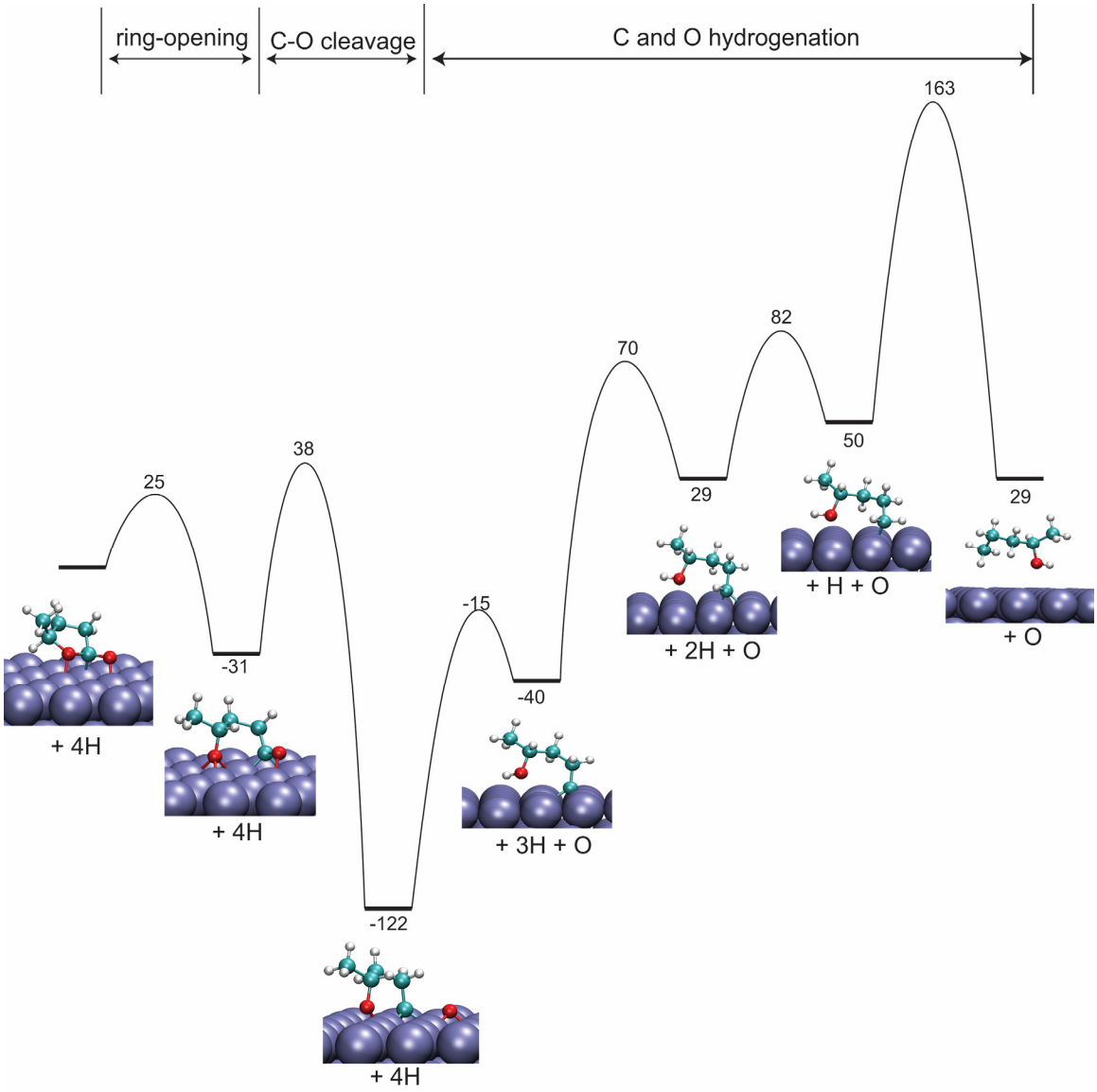

Figure 2 Energy profile calculations (kJ/mol) for the formation of 2-Pentanol from GVL.

The second pathway examined in this contribution is the formation of 2-pentanol. The first step in this reaction is the same formation of the ring-opened acyl intermediate $CH_3CH(O^*)\text{-}(CH_2)_2\text{-}C^*\text{-}O^*$. The subsequent step in this reaction is the direct deoxygenation of the intermediate to form $CH_3CH(O^*)\text{-}(CH_2)_2\text{-}C^*$ and an oxygen atom adsorbed on the surface. This deoxygenation step has an energy barrier of 69

kJ/mol and is exothermic (91 kJ/mol). The exothermicity of this step is due to the strong interaction of the oxygen atom with Ru(0001), and the newly formed α-Carbon strongly interacting with the Ru surface. The hydrogen-assisted deoxygenation has also been investigated in this case, where C(1)-O(1) bond breaking occurred after the hydrogenation of the O(1) Oxygen. The calculated true activation barrier is 24 kJ/mol (Figure S4), much lower than that of the direct deoxgenation shown in Figure 2. However, as shown in Figure 1, the hydrogenation step of this the O(1) atom has an activation barrier of 100 kJ/mol, which is higher than that for the direct deoxygenation (69 kJ/mol). Therefore, the direct deoxgenation is more likely to happen rather than the hydrogen-assisted deoxygenation. The subsequent steps in the formation of 2-pentanol are the hydrogenation of the second oxygen atom – O(2), which has an energy barrier of 107 kJ/mol, followed by three hydrogenation steps of the unsaturated α-Carbon, as shown in Figure 2. The rate-limiting step of these reactions is the third hydrogenation of the α-Carbon to completely break the Ru-C bond. This overall reaction has apparent activation energy of 163 kJ/mol. with an energy cost of 29 kJ/mol.

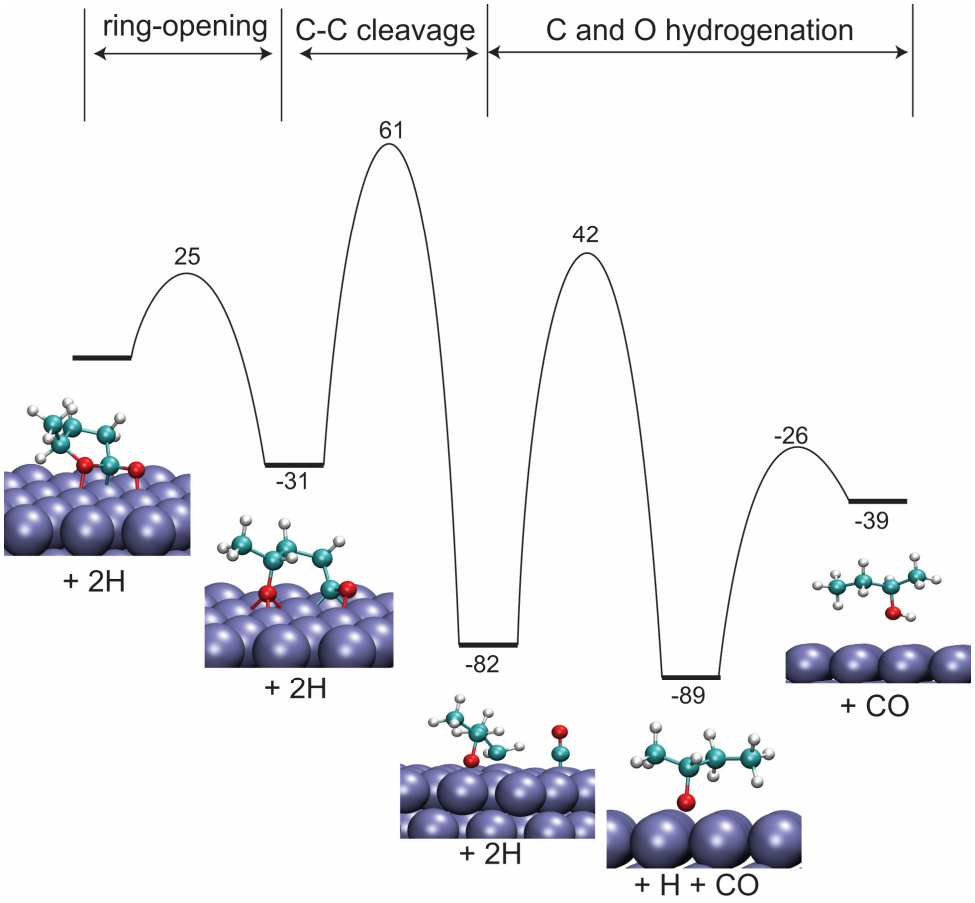

Figure 3 Energy profile calculations (kJ/mol) for the formation of 2-Butanol from GVL.

Next, we examined the reaction path for the conversion of GVL to 2-butanol. Figure 3 shows that this pathway involves a decarbonylation step of the acyl intermediate formed as a result of GVL ring opening. Decarbonylation of $CH_3CH(O^*)$-$(CH_2)_2$-C^*-O^* to yield $CH_3CH(O^*)$-CH_2-CH_2^* and carbon monoxide has an energy barrier of 92 kJ/mol and is exothermic (-51 kJ/mol). Once the $CH_3CH(O^*)$-CH_2-CH_2^* intermediate is formed, hydrogenation of the oxygen atom and the α-Carbon have true energy barriers of 124 kJ/mol and 63 kJ/mol, respectively. The rate-limiting step of forming 2-butanol is thus the decarbonylation of the acyl intermediate. Indeed, Rozenblit et al. have shown strong inhibition effect for forming 2-butanol when CO is introduced[24], which supports the conclusion that the direct decarbonylation of the ring-opened GVL is rate-limiting.

Now, we are in a position to compare all the reaction pathways. First, we note that the formation of 2-butanol has the lowest apparent barrier (61 kJ/mol), and can

be formed directly from GVL through a ring-opened acyl intermediate. This result is in line with the experimental results showing that 2-butanol is the most abundant product[24]. The above study also suggests that all products are primary and can be formed directly from the aforementioned acyl intermediate. Meanwhile, the moderate barrier for 1,4-PDO to form the same acyl intermediate (72 kJ/mol as indicated in Figure 1 by an arrow) suggests that, once 1,4-PDO forms, it can easily convert to 2-butanol and MTHF as well, which probably explains why the yield of 1,4-PDO is always very low[23,24]. Instead, due to the large activation barrier, formation of 2-pentanol should be very limited. Because of the thermal stability of the acyl intermediate and large activation barrier for the hydrogenation, the Ru surface may be covered mostly by the acyl species under the reaction condition. We have also calculated the adsorption energies of GVL and all the products on the Ru surface, which is summarized in Table 1. The adsorption energies are rather similar, which may suggest competitive adsorption of these species on the surface. Particularly, due to the large heat of adsorption on the Ru surface, 1,4-PDO may stay on the surface and undergo dehydrogenation to form other products, such as 2-BuOH, 2-PeOH and 2-MTHF, which is supported by the experimental observation of 2-BuOH, 2-MTHF, and 2-PeOH when feeding 1,4-PDO[24]. Iglesia et al. (*Kinetic and Mechanistic assessment of Alkanol/Alkanal Decarbonylation and Deoxygenation pathways of metal catalysts)* also showed that decarbonylation and hydrogenolysis of alkanols goes through dehydrogenation steps to activate the C-C bond vicinal to the terminal oxygen.

Table 1. Adsorption energy of GVL and all the products using the DFT-D3 method.

	GVL	1,4-PDO	2-PeOH	2-BuOH	2-MTHF
E_{ads} (kJ/mol)	-96	-113	-107	-98	-98

We do not present details of the formation of MTHF here since previous experiments over a Ru catalyst have shown that MTHF is a secondary product [24] and can be obtained from 1,4-PDO[22,23]. We have calculated the ring-closure reaction using the deoxygenated acyl species $CH_3CH(O^*)$-$(CH_2)_2$-C^* in Figure 2 as the initial structure, and found a very high activation barrier of 318 kJ/mol for this ring-closure

step, due to the fact that this ring closing requires the breaking of multiple C-Ru and O-Ru bonds. One possibility is that MTHF forms from $CH_3CH(O^*)$-$(CH_2)_2$-HC* in Figure 2 followed by ring closing and hydrogenation, because the hydrogenation of the C(1) carbon may weaken the interaction between C(1) and the Ru surface leading to reduced barrier for ring-closure. This unsaturated alcohol intermediate, $CH_3CH(O^*)$-$(CH_2)_2$-HC*, can be formed by deoxygenation of the acyl species $CH_3CH(O^*)$-$(CH_2)_2$-C*-O*; however, due to the smaller activation barrier for the competing C-C cleavage for decarbonylation to form $CH_3CH(O^*)$-$(CH_2)_2$ and sequentially hydrogenation, 2-BuOH may be more competitive as compared to formation of MTHF. So MTHF may not be formed through a direct transformation from GVL. Instead, MTHF should be formed via ring-closure of the same $CH_3CH(O^*)$-$(CH_2)_2$-HC* intermediate that is formed from dehydrogenation and hydrogenolysis of 1,4-PDO, followed by a hydrogenation step as described in Figure Sx. (I put the figure in dropbox.

Conclusion

In this study, we report a detailed reaction mechanism study for the conversion of GVL on a ruthenium catalyst. Our calculations suggest that 1,4-PDO, 2-BuOH and 2-PeOH can be formed through a common surface intermediate, but their rate-limiting step varies differently from hydrogenation for 1,4-PDO and 2-PeOH to decarbonylation for 2-BuOH, the latter has the smallest activation barrier. These results agree with previous experimental results reported in the literature and can be used as a guide for design of new catalysts with tailored reaction selectivity. For example, if 1,4-PDO and MTHF were the target molecules, one option would be to design bimetallic catalysts that retain a high activity for ring opening, such as Ru, but promote the hydrogenation step, such as using Pt or Pd.

Acknowledgements

This contribution was identified by Hongliang Xin (Virginia Polytechnic Institute and State University) as the Best Presentation in the session “Computational Chemistry for Energy Application” of the 2016 ACS Fall National Meeting in Philadelphia, PA. The authors also appreciate valuable discussion with Drs. Tawan Sooknoi and Qiaohua

Tan. The authors thank the support from U.S. Department of Energy, DOE/EPSCOR (Grant DESC0004600). The DFT calculations were performed at the National Energy Research Scientific Computing Center (NERSC) and the OU Supercomputing Center for Education & Research (OSCER) at the University of Oklahoma.

Reference

(1) Vispute, T. P.; Zhang, H. Y.; Sanna, A.; Xiao, R.; Huber, G. W. Renewable Chemical Commodity Feedstocks from Integrated Catalytic Processing of Pyrolysis Oils. *Science* **2010**, *330*, 1222-1227.

(2) Huber, G. W.; Cortright, R. D.; Dumesic, J. A. Renewable alkanes by aqueous-phase reforming of biomass-derived oxygenates. *Angew Chem Int Edit* **2004**, *43*, 1549-1551.

(3) Davda, R. R.; Shabaker, J. W.; Huber, G. W.; Cortright, R. D.; Dumesic, J. A. A review of catalytic issues and process conditions for renewable hydrogen and alkanes by aqueous-phase reforming of oxygenated hydrocarbons over supported metal catalysts. *Appl Catal B-Environ* **2005**, *56*, 171-186.

(4) Christensen, E.; Yanowitz, J.; Ratcliff, M.; McCormick, R. L. Renewable Oxygenate Blending Effects on Gasoline Properties. *Energ Fuel* **2011**, *25*, 4723-4733.

(5) Alonso, D. M.; Bond, J. Q.; Dumesic, J. A. Catalytic conversion of biomass to biofuels. *Green Chem* **2010**, *12*, 1493-1513.

(6) Corma, A.; Iborra, S.; Velty, A. Chemical routes for the transformation of biomass into chemicals. *Chem Rev* **2007**, *107*, 2411-2502.

(7) Van de Vyver, S.; Roman-Leshkov, Y. Emerging catalytic processes for the production of adipic acid. *Catal Sci Technol* **2013**, *3*, 1465-1479.

(8) Fegyverneki, D.; Orha, L.; Lang, G.; Horvath, I. T. Gamma-valerolactone-based solvents. *Tetrahedron* **2010**, *66*, 1078-1081.

(9) Wettstein, S. G.; Alonso, D. M.; Chong, Y. X.; Dumesic, J. A. Production of levulinic acid and gamma-valerolactone (GVL) from cellulose using GVL as a solvent in biphasic systems. *Energ Environ Sci* **2012**, *5*, 8199-8203.

(10) Bond, J. Q.; Alonso, D. M.; Wang, D.; West, R. M.; Dumesic, J. A. Integrated Catalytic Conversion of gamma-Valerolactone to Liquid Alkenes for Transportation Fuels. *Science* **2010**, *327*, 1110-1114.

(11) Palkovits, R. Pentenoic Acid Pathways for Cellulosic Biofuels. *Angew Chem Int Edit* **2010**, *49*, 4336-4338.

(12) Wright, W. R. H.; Palkovits, R. Development of Heterogeneous Catalysts for the Conversion of Levulinic Acid to gamma-Valerolactone. *Chemsuschem* **2012**, *5*, 1657-1667.

(13) Alonso, D. M.; Wettstein, S. G.; Dumesic, J. A. Gamma-valerolactone, a sustainable platform molecule derived from lignocellulosic biomass. *Green Chem* **2013**, *15*, 584-595.

(14) Mehdi, H.; Fabos, V.; Tuba, R.; Bodor, A.; Mika, L. T.; Horvath, I. T. Integration of homogeneous and heterogeneous catalytic processes for a multi-step

conversion of biomass: From sucrose to levulinic acid, gamma-valerolactone, 1,4-pentanediol, 2-methyl-tetrahydrofuran, and alkanes. *Top Catal* **2008**, *48*, 49-54.

(15) Resasco, D. E.; Sitthisa, S.; Faria, J.; Prasomsri, T.; Ruiz, M. P.: 5. Furfurals as chemical platform for biofuels production. In *Solid Waste as a Renewable Resource: Methodologies*; Albanese, A. J. F., Ruiz, M. P., Eds., 2011; pp 103.

(16) Lange, J. P.; van der Heide, E.; van Buijtenen, J.; Price, R. Furfural—a promising platform for lignocellulosic biofuels. *ChemSusChem* **2012**, *5*, 150-166.

(17) Xing, R.; Qi, W.; Huber, G. W. Production of furfural and carboxylic acids from waste aqueous hemicellulose solutions from the pulp and paper and cellulosic ethanol industries. *Energ Environ Sci* **2011**, *4*, 2193-2205.

(18) Bui, T. V.; Crossley, S.; Resasco, D. E. C-C Coupling for Biomass - Derived Furanics Upgrading to Chemicals and Fuels. *Chemicals and Fuels from Bio-Based Building Blocks* **2016**, 431-494.

(19) Bui, L.; Luo, H.; Gunther, W. R.; Roman-Leshkov, Y. Domino Reaction Catalyzed by Zeolites with BrOnsted and Lewis Acid Sites for the Production of -Valerolactone from Furfural. *Angew Chem Int Edit* **2013**, *52*, 8022-8025.

(20) Bond, J. Q.; Alonso, D. M.; West, R. M.; Dumesic, J. A. gamma-Valerolactone Ring-Opening and Decarboxylation over SiO2/Al2O3 in the Presence of Water. *Langmuir* **2010**, *26*, 16291-16298.

(21) Christian, R. V.; Brown, H. D.; Hixon, R. M. Derivatives of Gamma-Valerolactone, 1,4-Pentanediol and 1,4-Di-(Beta-Cyanoethoxy)-Pentane. *J Am Chem Soc* **1947**, *69*, 1961-1963.

(22) Geilen, F. M. A.; Engendahl, B.; Harwardt, A.; Marquardt, W.; Klankermayer, J.; Leitner, W. Selective and Flexible Transformation of Biomass-Derived Platform Chemicals by a Multifunctional Catalytic System. *Angew Chem Int Edit* **2010**, *49*, 5510-5514.

(23) Al-Shaal, M. G.; Dzierbinski, A.; Palkovits, R. Solvent-free gamma-valerolactone hydrogenation to 2-methyltetrahydrofuran catalysed by Ru/C: a reaction network analysis. *Green Chem* **2014**, *16*, 1358-1364.

(24) Rozenblit, A.; Avoian, A. J.; Tan, Q.; Sooknoi, T.; Resasco, D. E. Reaction mechanism of aqueous-phase conversion of γ-valerolactone (GVL) over a Ru/C catalyst. *Journal of Energy Chemistry* **2016**, *25*, 1008-1014.

(25) Du, X. L.; Bi, Q. Y.; Liu, Y. M.; Cao, Y.; He, H. Y.; Fan, K. N. Tunable copper-catalyzed chemoselective hydrogenolysis of biomass-derived gamma-valerolactone into 1,4-pentanediol or 2-methyltetrahydrofuran. *Green Chem* **2012**, *14*, 935-939.

(26) Kresse, G.; Furthmuller, J. Efficient iterative schemes for ab initio total-energy calculations using a plane-wave basis set. *Phys Rev B* **1996**, *54*, 11169-11186.

(27) Perdew, J. P.; Burke, K.; Ernzerhof, M. Generalized gradient approximation made simple. *Phys Rev Lett* **1996**, *77*, 3865-3868.

(28) Blochl, P. E. Projector Augmented-Wave Method. *Phys Rev B* **1994**, *50*, 17953-17979.

(29) Kresse, G.; Joubert, D. From ultrasoft pseudopotentials to the projector augmented-wave method. *Phys Rev B* **1999**, *59*, 1758-1775.

(30) Grimme, S.; Antony, J.; Ehrlich, S.; Krieg, H. A consistent and accurate ab initio parametrization of density functional dispersion correction (DFT-D) for the 94 elements H-Pu. *J Chem Phys* **2010**, *132*, 154104.

(31) Deimel, P. S.; Bababrik, R. M.; Wang, B.; Blowey, P. J.; Rochford, L. A.; Thakur, P. K.; Lee, T. L.; Bocquet, M. L.; Barth, J. V.; Woodruff, D. P.; Duncan, D. A.; Allegretti, F. Direct quantitative identification of the "surface trans-effect". *Chem Sci* **2016**, *7*, 5647-5656.

(32) Henkelman, G.; Uberuaga, B. P.; Jonsson, H. A climbing image nudged elastic band method for finding saddle points and minimum energy paths. *J Chem Phys* **2000**, *113*, 9901-9904.

(33) Henkelman, G.; Jonsson, H. Improved tangent estimate in the nudged elastic band method for finding minimum energy paths and saddle points. *J Chem Phys* **2000**, *113*, 9978-9985.

(34) Yin, A. X.; Liu, W. C.; Ke, J.; Zhu, W.; Gu, J.; Zhang, Y. W.; Yan, C. H. Ru Nanocrystals with Shape-Dependent Surface-Enhanced Raman Spectra and Catalytic Properties: Controlled Synthesis and DFT Calculations. *J Am Chem Soc* **2012**, *134*, 20479-20489.

(35) van Santen, R. A.; Tranca, I. How molecular is the chemisorptive bond? *Phys Chem Chem Phys* **2016**, *18*, 20868-20894.

(36) Mironenko, A. V.; Gilkey, M. J.; Panagiotopoulou, P.; Facas, G.; Vlachos, D. G.; Xu, B. J. Ring Activation of Furanic Compounds on Ruthenium-Based Catalysts. *J Phys Chem C* **2015**, *119*, 6075-6085.